C.P. No. 88
(14,192)
A.R.C. Technical Report

MINISTRY OF SUPPLY

AERONAUTICAL RESEARCH COUNCIL

CURRENT PAPERS

Fatigue Tests on Typical Two Spar Light Alloy Structures (Meteor 4 Tailplanes) under Reversed Loading

By

K. D. Raithby, B.Sc., A.F.R.Ae.S.

LONDON: HER MAJESTY'S STATIONERY OFFICE

1952

Four Shillings Net

C.P. No.88

Report No. Structures 108

May, 1951

ROYAL AIRCRAFT ESTABLISHMENT

Fatigue Tests on Typical Two Spar Light Alloy Structures (Meteor 4 Tailplanes) under Reversed Loading

by

K.D. Rainsby, B.Sc., A.F.R.Ae.S.

SUMMARY

Results are given for fatigue tests on six Meteor 4 tailplanes, vibrated in flexure under simple reversed loading, ranging from ± 10% to ± 30% of the static failing load. Corresponding endurances varied from about 5×10^6 to 0.06×10^6 cycles, for complete failure of a spar boom. In each test the alternating load was kept constant, although progressive skin cracking caused a considerable change in alternating stress at the section where eventual failure of the spar boom occurred.

The test results are discussed in relation to the establishment of endurance curves for a typical two spar structure.

LIST OF CONTENTS

LIST OF APPENDICES

LIST OF TABLES

LIST OF ILLUSTRATIONS

1 Introduction

In order to provide information on the fatigue strength of a typical structure, an extensive test programme has been initiated on Meteor 4 tailplanes. These are regarded as being generally representative of a two spar light alloy wing, but without the severe load or stress concentrations which occur at wing spar joints.

This Report gives the results of fatigue tests on six tailplanes under simple reversed loading ranging from ±10% to ±30% of the static failing load. An approximate method is suggested for correcting the results to take account of the considerable change in stress distribution caused by extensive cracking of the interspar skins.

Other tests, under different loading conditions, will be reported separately.

2 Structural Features of the Meteor 4 Tailplane

The Meteor 4 tailplane, shown diagrammatically in Fig. 1, is of two spar light alloy construction, with diaphragm type ribs and with top and bottom skins stiffened by stringers which are discontinuous at the ribs. The spar booms are L section extrusions in L40 material, continuous along the span. The front spar booms are cranked back at about 6 in. outboard of the root attachment points.

There are four tailplane root attachment points, two on each spar. Each attachment point comprises a single bolt passing through the spar web at about 5 in. from the tailplane centre line. The spar webs are locally reinforced with channel section stiffeners and steel doubler plates.

Over the inboard half of the tailplane, the skins are of aluminium alloy (D.T.D.390) while outboard they are of high tensile steel (D.T.D.138). There are a number of unreinforced access holes cut in the top and bottom skins near the root attachments. It was found that these holes caused early skin cracking in the fatigue tests, which led to an appreciable increase in spar boom stresses.

3 Preliminary Static Strength Tests

Static strength tests were made on three tailplanes to determine the mean failing load on which to base the fatigue tests. Each specimen failed by compression of the rear spar top boom between ribs 2 and 3, approximately 11.5 in. from the centre line.

A summary of the results of the three tests is given in Table I. Strain gauge readings taken during the static tests were used to estimate the proportions of the total bending moment carried by each spar and by the skin. The spar boom stresses were then calculated from Engineers' simple bending theory. Compressive stresses are based on the gross area of the boom and part of the web; tensile stresses are based on the net area, allowance being made for rivet holes etc.

4 Loading Conditions for Fatigue Tests

4.1 Load Distribution

For a conventional wing the spanwise load distribution in flight would be approximately proportional to the chord and, in an ideal case, the spars would be tapered to give uniform stress along the span.

In Fig. 2, approximate spanwise distribution curves of direct stress for the Meteor tailplane are given for various loading conditions. The stresses are based on gross spar boom areas (i.e. without allowance for rivet holes) and were calculated from the bending moment curves appropriate to each loading condition.

With a distributed load proportional to the chord, the spar stresses reach a maximum at the point where failure occurred in the static strength tests, but fall away rapidly with distance along the span, due to the small amount of taper on the spar booms. A single load near the tip, however, while still giving maximum stress at the point of static failure, gives a much closer approximation to the condition of uniform stress distribution in an ideal wing. This type of loading is closely represented by vibrating the tailplane at its natural frequency with a relatively heavy mass near the tip.

For the present series of fatigue tests each tailplane was vibrated by an exciter mounted near the tip. The exciter used for the lower ranges of loading weighed 35 lb and that used for the higher ranges 97 lb. Corresponding shear and bending moment curves, for unit bending moment at the section where failure occurred in the static tests, are given in Fig. 3. These curves are based on an estimated structure weight distribution and on measured displacements (see Fig. 4). Under the test conditions the ratio of shear stress in the webs to direct stress in the spar booms is low, but this is considered unimportant, as it is likely that fatigue failures on such a structure will usually be associated with bending.

4.2 Range of Loading

Tests were made on six tailplanes under various alternating loads. In each test the mean load was approximately zero, although in fact there was a small mean load due to the weight of the tailplane and test rig.

The alternating load and mean load for each test are given in Table II. The loads are expressed as percentages of the equivalent load that would produce a bending moment at 11.5 in. from the tailplane centreline* equal to the mean bending moment at failure in the static strength tests. Corresponding alternating stresses in the spar booms at the beginning of the test, calculated from the applied bending moment, are given in Table III.

The alternating load was kept the same throughout each test, irrespective of any change in stiffness or stress distribution.

5 Method of Test

Each tailplane was attached to a steel anchorage structure by the root attachment bolts and was vibrated in flexure close to its natural frequency. Strain gauges on the spar booms and skin were used to measure the applied bending moment and to check the distribution of direct stress between skin and spars near the root.

The amplitude of vibration was adjusted to give strain gauge readings corresponding to the required range of bending moment. The test was continued until failure of one of the spar booms occurred.

The method of test is given in more detail in Appendix I.

---

* Position of failure in static strength tests.

6 Discussion of Test Results

6.1 Skin Cracks and Their Effect on Spar Boom Stresses

Cracking of the intersp[illegible] skins started at an early stage (usually at about 1/10 of the total life of the tailplane). At first the cracks spread slowly but later spread more rapidly until they reached a boundary such as a rivet hole or the edge of the sheet. In many cases complete failure of the interspar skin occurred. As a result of the skin cracks, the spar boom stresses increased, by an amount depending on the position and extent of the cracks.

The development of typical skin cracks is illustrated in Fig. 5, in which the effective width of skin, expressed as a proportion of the distance between spars, is plotted against number of cycles. Corresponding changes in spar boom stresses (deduced from strain gauge readings) are shown in Fig. 6. Typical skin failures are shown in Figs. 8 and 9. Most of the skin failures originated either at unreinforced access holes in top or bottom skin near the root, or at cracks associated with local bending of the skin under compressive load where stringers were discontinuous across ribs.

6.2 Rivet Failures

Rivet failures often occurred at an early stage along the chordwise lap joint between the steel and aluminium alloy skins at rib 5. At later stages some failures of skin to spar boom rivets occurred, usually after skin cracks had appeared

Typical rivet failures may be seen in Figs. 8 to 10.

6.3 Spar Failure

Each test was continued until complete failure of a spar boom occurred. The results are given in Table II and are plotted in Fig. 7 (curve 1). Typical failures are illustrated in Fig. 11. All the failures appeared to start from rivet holes in the spar flange. It will be noted that in two tests, failure occurred in the front spar, although the nominal stress was only about 70% of that in the rear spar. It is probable that failure of the front spar was due largely to residual stresses associated with the cranking of the boom during manufacture.

7 Corrected Endurance Curves

In order to interpret the results in terms of endurance curves for a typical structure, it is necessary to consider what the endurance would have been (a) if extensive skin cracking had not occurred and (b) if the tension boom of the rear spar had developed its full strength in the static strength tests.

The development of skin cracking resulted in a considerable increase in spar boom stresses for a given load. Assuming that the cumulative damage rule holds good, it is possible to estimate what the endurance would have been if the alternating stress in the spars had remained constant. Using the method given in Appendix II, a corrected endurance curve has been derived for the rear spar and is shown in Fig. 7 (curve 2). Also plotted on this curve is the result of a previous test,[1] in which the alternating stress in the rear spar was kept constant throughout.

Curve 3 in Fig. 7 is obtained by plotting the corrected endurance curve in terms of the calculated tensile strength of the rear spar instead

of the static failing load of the tailplane. The tensile strength was based on the specification minimum ultimate strength of 27 tons/in^2 for L40 material. The calculated tensile stress at failure in the static strength tests was only 22.5 tons/in^2. It will be seen that curve 3 lies very close to the original curve 1.

8 Effective Stress Concentration in Rear Spar Boom at Point of Failure

An approximation to the effective stress concentration in the rear spar boom at the point of failure can be made by comparing the corrected endurance curve (based on the tensile strength of the boom) with the endurance curve for reversed axial loading on polished test pieces. The effective fatigue stress concentration factor is given by the ratio of alternating stress in polished bar test to alternating stress in tailplane spar for failure in a given number of cycles, the stress in each case being based on the net area. There is little existing data on the fatigue strength of L40 material, but there are a large number of test results for American 14S-T material. This has a higher ultimate strength than L40 but the ratio of fatigue strength to ultimate strength is about the same. Endurance values for reversed axial stress, expressed as a percentage of the ultimate strength, have been extrapolated from curves given in Ref. 2 and are plotted in Fig. 7.

The effective stress concentration factor of the spar boom varies from about $3\frac{1}{2}$ at 10^7 cycles (corresponding to $\pm 8.2\%$ ultimate in the rear spar) to just under 2 at 10^5 cycles ($\pm 26\%$ ultimate in the rear spar).

9 Conclusions

Fatigue tests on six Meteor 4 tailplanes at approximately zero mean load show that, under alternating loads between $\pm 10\%$ and $\pm 30\%$ of the static failing load, the endurance varies from 5×10^6 to 0.06×10^6 cycles, for complete failure of a spar boom. Failure usually occurs in the rear spar, but sometimes in the front spar. Skin cracking and rivet failures occur at an appreciably lower number of cycles than are required to produce failure of either spar.

If the alternating load is expressed as a percentage of the calculated tensile strength of the rear spar instead of the same percentage of the static strength of the complete tailplane, the endurance is roughly halved.

The endurance would probably be nearly doubled, however, if extensive skin cracking did not occur. This skin cracking is mainly due to

(a) Stress concentrations at access holes in the skin.

(b) Local bending of the skin associated with discontinuous stringers.

The effective fatigue stress concentration factor in the rear spar boom at the point of failure varies from about $3\frac{1}{2}$ for 10^7 cycles at an alternating stress of $\pm 8.2\%$ ultimate to just under 2 for 10^5 cycles at $\pm 26\%$ ultimate.

REFERENCES

No.	Author	Title etc
1	J.K. Oaks	Fatigue Test on Meteor Tailplane. ARC 13,061 January, 1950
2	L.R. Jackson, L.J. Grover and R.C Mc Master	Survey of Available Information on the Behaviour of Aircraft Materials and Structures under Repeated Load. Report to the War Metallurgy Committee on Survey Project No. SP-27. Battelle Memorial Institute December, 1945

APPENDIX I

Method of Test

1 Mounting of Test Specimen

Steel channel sections were bolted through the webs to the front face of the front spar and the rear face of the rear spar, using the holes provided for the attachment of the tailplane to the fin. Thin washers were inserted between the steel channels and the spar webs so that no lateral support was given to the spars by the steel channels. The latter were bolted to an anchorage rig which was attached either to a small test frame or to a concrete plinth with embedded steel rails.

A tailplane rigged for test is shown in Fig. 12.

2 Method of Excitation

For all tests, a double rotating out of balance mass exciter, giving a simple harmonic vertical force, was bolted between the spars at rib 8 on one side of the tailplane, with an equal dead weight on the other side. For tailplanes 4 and 7 an exciter weighing 35 lb was used, giving a frequency of vibration of about 18 c.p.s. For the other tailplanes a larger exciter was used. This weighed 97 lb and gave a frequency of about 12 c.p.s.

3 Strain Gauges

Electrical resistance strain gauges of the British Thermostat 200 ohm type were cemented to spar booms and skin either at 5.5 in. or at 11.5 in. from the tailplane centre line, as indicated in Fig. 1. The gauges were used primarily to measure the applied bending moment in the fatigue tests, but also to determine the approximate distribution of direct stress between spars and skin. In one test (tailplane No. 5) gauges were also cemented to the skin at various sections along the span to check the bending moment distribution (see Fig. 3).

The gauges formed one or more arms of a Wheatstone's bridge circuit and were used in conjunction with a Tinsley Strain Bridge and Selector Switch. In some cases, dummy unstrained gauges, mounted on similar material, were connected into the bridge circuit to compensate for changes in resistance due to temperature variation. In other cases, dummy gauges were dispensed with and the active gauges were connected in pairs (e.g. rear spar top and bottom boom) to form adjacent arms of the bridge.

Changes of resistance were measured on a cathode ray oscilloscope connected across the bridge. Under dynamic loading, the gauge signals gave a sinusoidal trace on the screen, the height of the wave being proportional to the total change of resistance. A rotary chopping switch, in series with the oscilloscope, was used to interrupt the gauge signal to give a continuously visible reference line on the screen.

At various stages throughout each test, the gauges were calibrated statically by applying dead load to the tailplane to cover the required range of bending moment.

4 Displacements

In each test the tip amplitude was measured by means of small tapered scales attached to each tip, so that when the tailplane was vibrating, the point where the image of the upper edge of the scale crossed that of the lower edge gave a direct reading of the total amplitude.

Measurements were also made at various points along the span, using pencils attached to the tailplane, in order to determine the mode of vibration. The resultant mode is plotted in Fig. 4. It will be noted that the difference in exciter weight appears to have little effect on the shape.

APPENDIX II

Derivation of Corrected Endurance Curves for Rear Spar

1 Notation

The following notation is used:-

f_1 = initial alternating stress in rear spar.

f_2 = final " " " " "

N_1 = endurance under constant alternating stress of f_1

N_2 = " " " " " " f_2

n_1 = No. of cycles actually applied at alternating stress f_1

n_2 = No. of cycles actually applied at alternating stress f_2

$N = n_1 + n_2$ = total number of cycles to failure in actual tailplane test, with initial alternating stress f_1.

N' = total no. of cycles to failure if initial alternating stress had been f_2 instead of f_1.

2 Assumptions

(i) The stress changes suddenly from f_1 to f_2.

(ii) It is assumed that the cumulative damage rule holds good. This may be expressed as follows:-

$$\frac{n_1}{N_1} + \frac{n_2}{N_2} = 1 \qquad (1)$$

(iii) Between the limits f_1 and f_2, the mean slope of the corrected endurance curve is the same as the mean slope of the uncorrected curve, when plotted on a log-scale.

This gives

$$\frac{N_1}{N_2} = \frac{N}{N'} \qquad (2)$$

3 Corrected Curve

From strain gauge readings taken during the tailplane tests, the value of f_2/f_1 can be deduced, hence from Fig. 7, Curve 1, the value of $\frac{N}{N'}$ can be determined.

From (1) and (2)

$$\frac{n_1}{N_1} + \frac{n_2}{N_1} \times \frac{N}{N'} = 1$$

Hence

$$N_1 = n_1 + \frac{N}{N'} \times n_2 \qquad (3)$$

and

$$N_2 = n_2 + \frac{N'}{N} \times n_1 \qquad (4)$$

Values of N_1 and N_2 for each test result are plotted in Curve 2 on Fig. 7.

TABLE I

Results of Static Strength Tests

Tail-plane No.	Serial No.	B.M. at Failure (lb in)	Estimated Direct Stress in Spar Boom at Failure (lb/in^2)			
			F.S. Top (compres-sion)	F.S. Bottom (tension)	R.S. Top (compres-sion)	R.S. Bottom (tension)
1	S4 C5 350104	365,000	44,000	42,500	60,000	52,000
2	366712	352,000	42,500	41,000	58,000	50,000
3	366707	348,000	42,000	40,500	57,500	49,500
Mean		355,000	43,000	41,500	58,500	5 ,500

* Stresses given are maximum stresses in boom at point of failure, i.e 11.5 in. from centreline. Compressive stresses are based on gross area; tensile stresses on net area

TABLE II

Results of Fatigue Tests

Tail-plane No.	Serial No.	Alternating Load % of S F.L.*	Mean Load % of S.F.L.*	No. of cycles to failure of spar boom	Position of Spar Boom Failure
4	S4 C5 366680	±10	0.8	6.44 x 10^5	Port rear top at rib 2, 6.7 in. from ℄
7	366679	±10.5	0.8	3.33 x 10^6	Port rear bottom at rib 2
5	366711	±20	2.5	0.515 x 10^6	Stbd rear top at rib 2
8	366759	±20	2.5	0.323 x 10^6	Port front top 11.5 in. from ℄
6	366682	±30	2.5	0.054 x 10^6	Port rear top at rib 2
10	366752	±30	2.5	0.065 x 10^6	Stbd front top 8.5 in. from ℄

* S.F.L. = equivalent static load that would give a bending moment of 355,000 lb.in. at 11.5 in. from centreline, i.e. mean bending moment at failure in static strength tests

TABLE III

Estimated Spar Boom Stresses at Beginning of Test

Tail-plane No.	Alternating Load % of S.F.L.	Alternating stress* lb/in^2			
		At 11.5 in. from ℄		At Rib 2(7 in. from ℄)	
		F.S.	R.S.	F.S.	R.S.
4	±10	±3500	±5100	±3700	±5000
7	±10.5	±3700	±5400	±3900	±5300
5	±20	±7000	±10200	±7400	±10000
8	±20	±7000	±10200	±7400	±10000
6	±30	±10500	±15300	±11100	±15000
10	±30	±10500	±15300	±11100	±15000

* Maximum stress in boom, based on net area (i.e. allowing for rivet holes etc). No stress concentration factor included.

Wt.2078.CP88.K3. Printed in Great Britain.

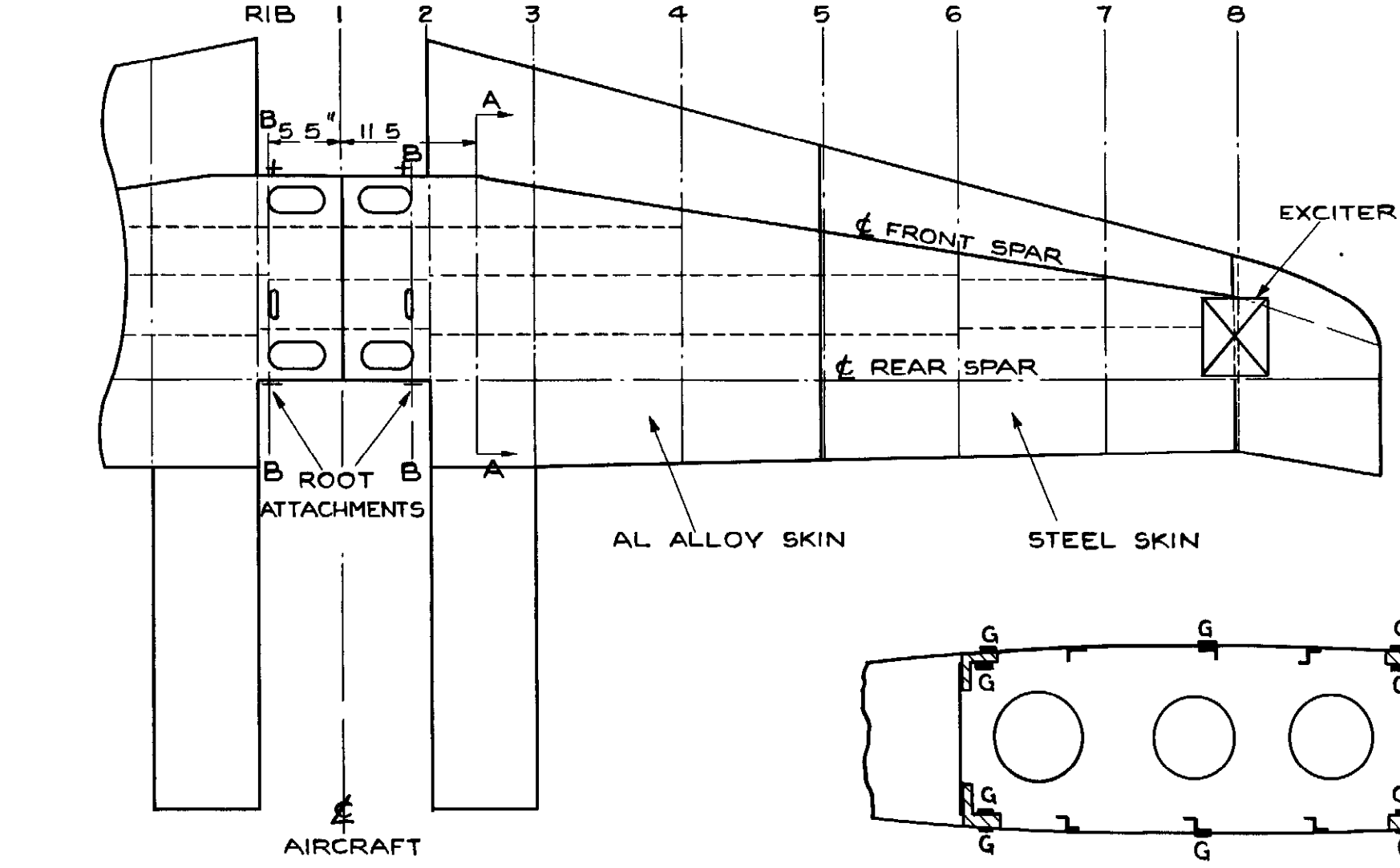

STRAIN GAUGE READINGS TAKEN AT SECTION AA OR BB ON PORT & STBD. SIDES

SECTION AA SHOWING TYPICAL STRAIN GAUGE POSITIONS (MARKED G)

FIG.1 GENERAL ARRANGEMENT OF TEST SPECIMEN

FIG.1

FIG.2

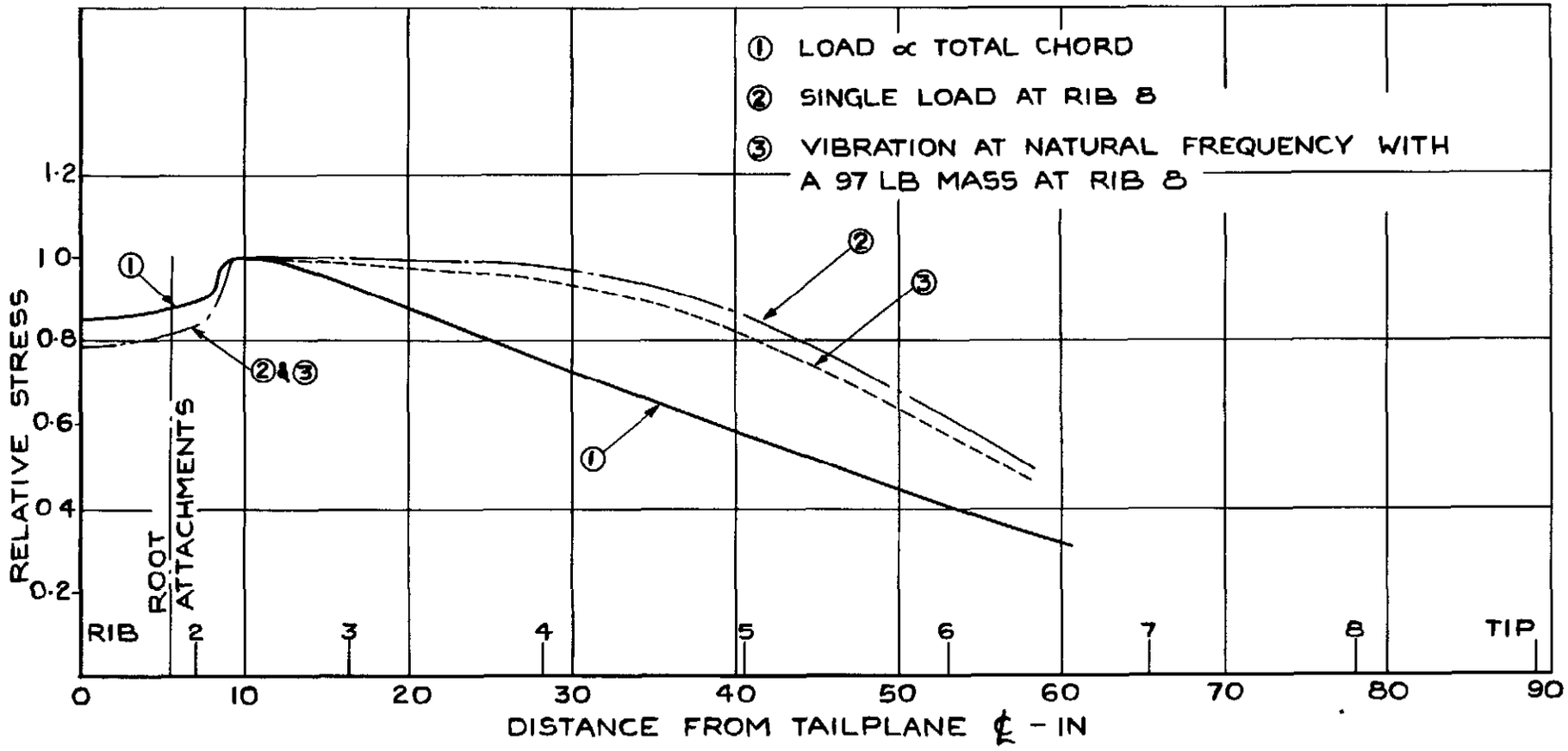

FIG.2. APPROXIMATE SPANWISE DISTRIBUTION OF DIRECT STRESS IN SPAR BOOMS
(UNIT STRESS AT 115 IN. FROM ℄)

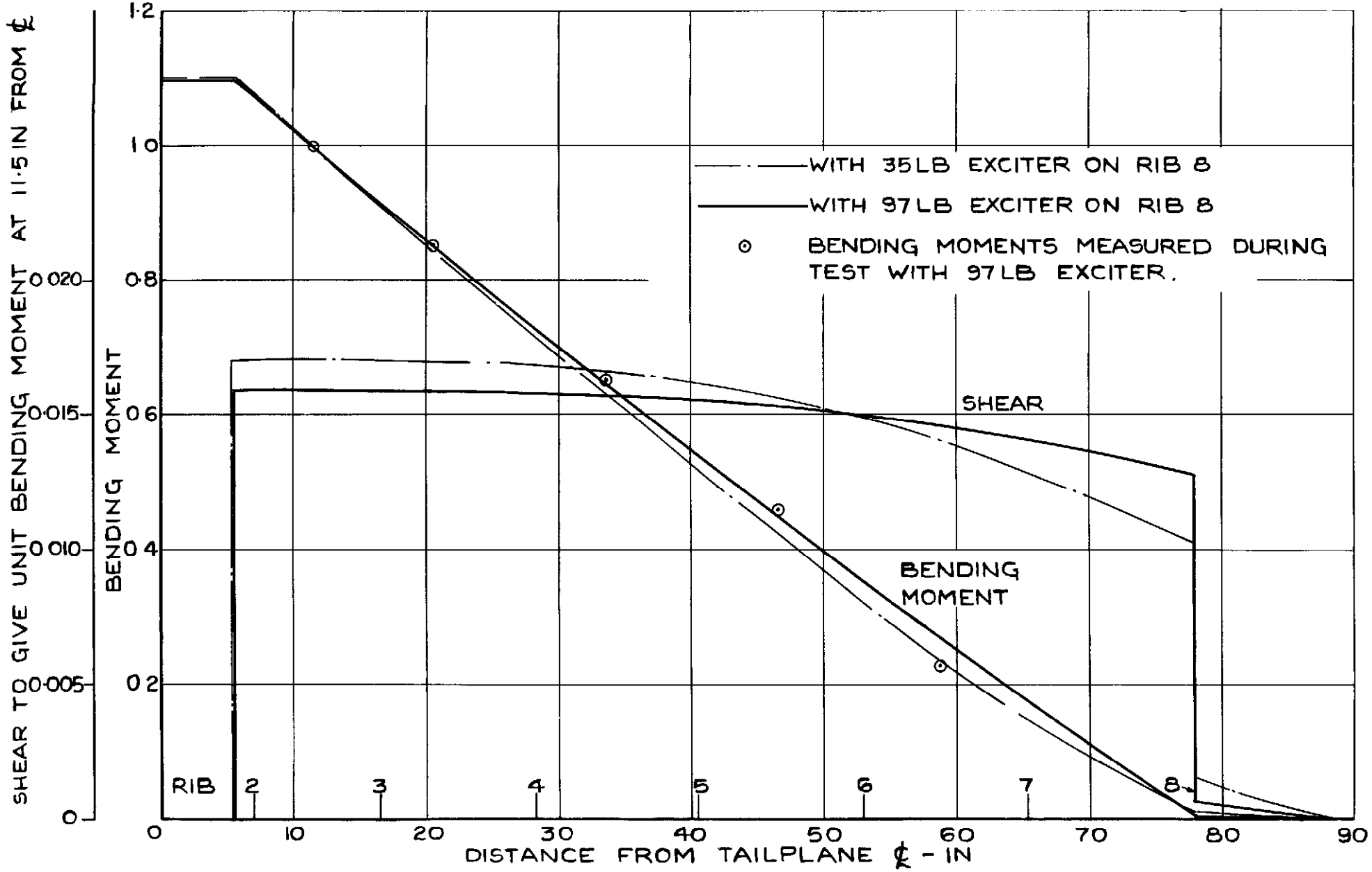

FIG. 3. SHEAR AND BENDING MOMENT CURVES
(UNIT B.M AT 11·5 IN FROM ℄)

FIG.3

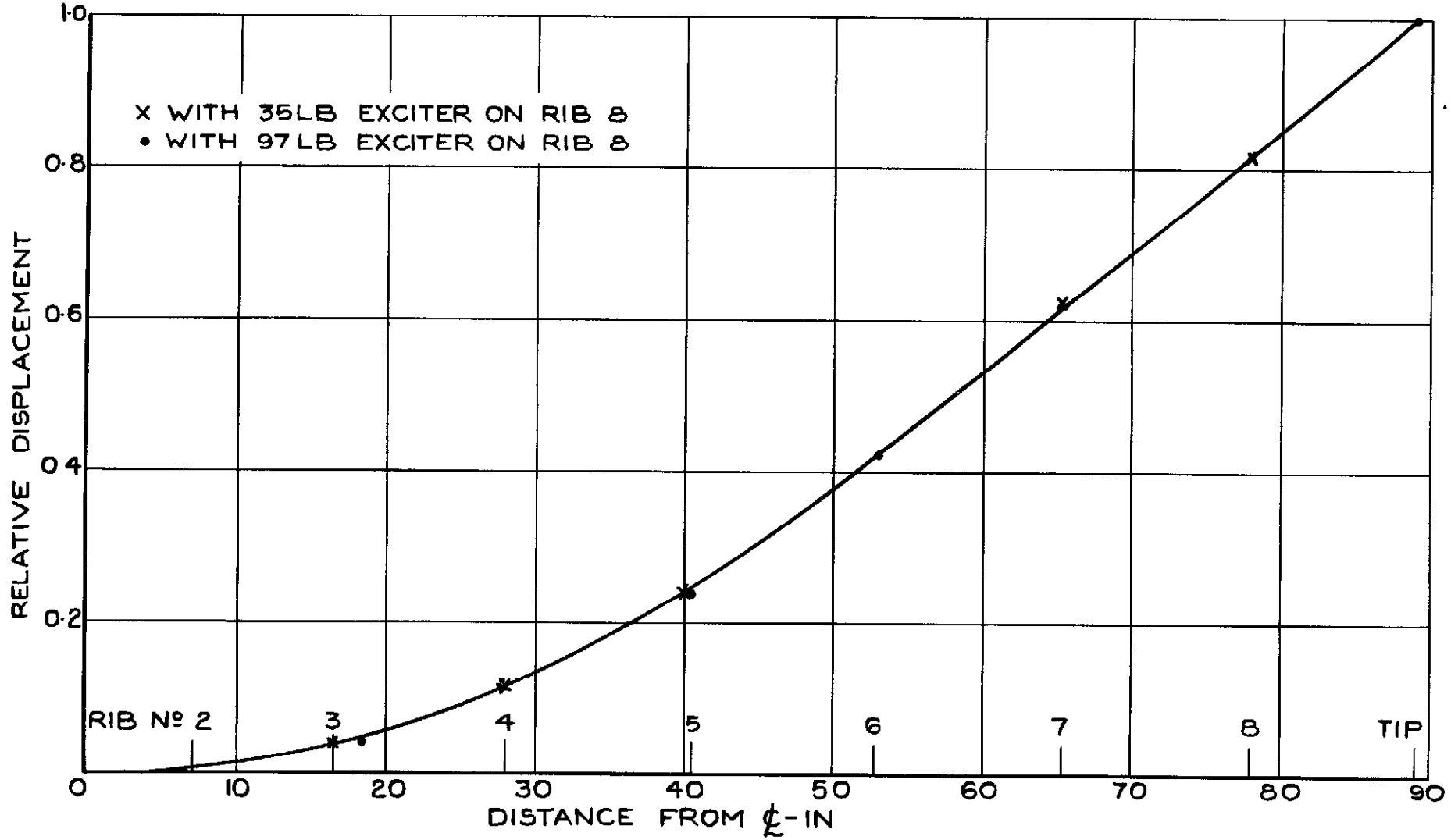

FIG.4. RELATIVE DISPLACEMENTS.

FIG.4

FIG.5&6

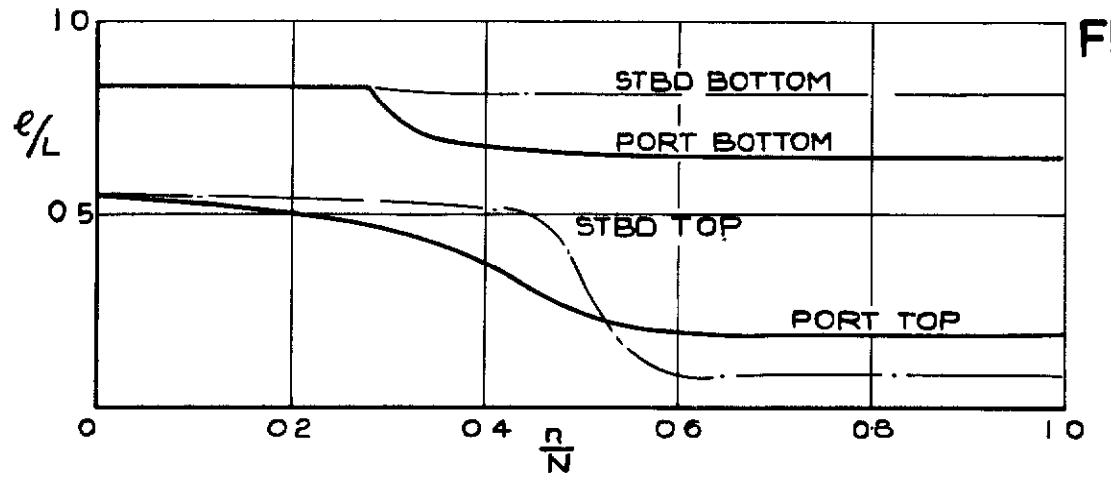

e = EFFECTIVE WIDTH OF SKIN AFTER n CYCLES
L = DISTANCE BETWEEN SPARS
N = Nº OF CYCLES TO FAILURE OF SPAR BOOM

FIG.5. DEVELOPMENT OF SKIN CRACKS AT RIB 2
(TAILPLANE Nº 8.)

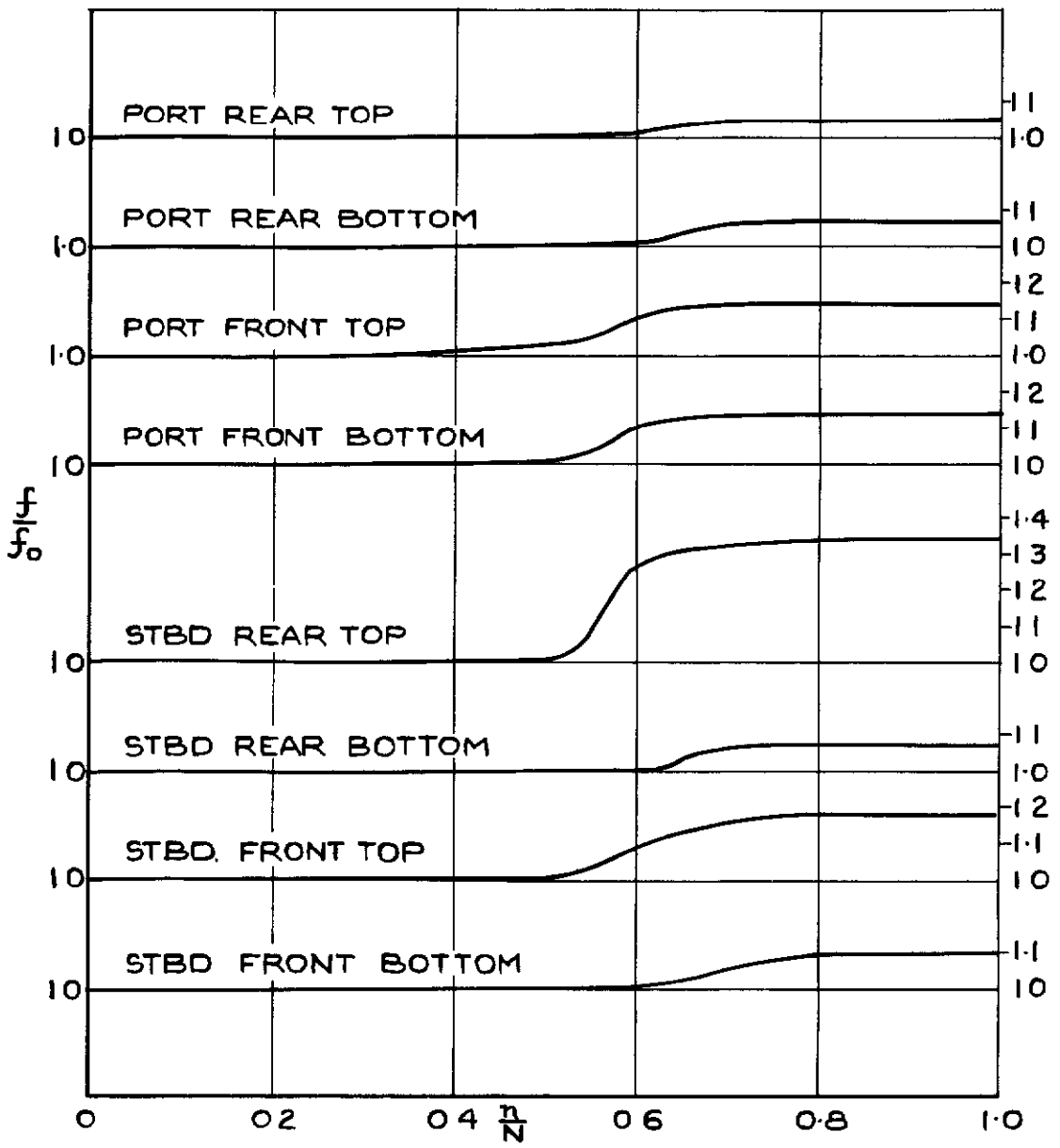

f = SPAR BOOM STRESS AFTER n CYCLES
f_0 = SPAR BOOM STRESS AT BEGINNING OF TEST

FIG.6 VARIATION OF SPAR BOOM STRESSES WITH Nº OF CYCLES AT RIB 2.
(TAILPLANE Nº 8)

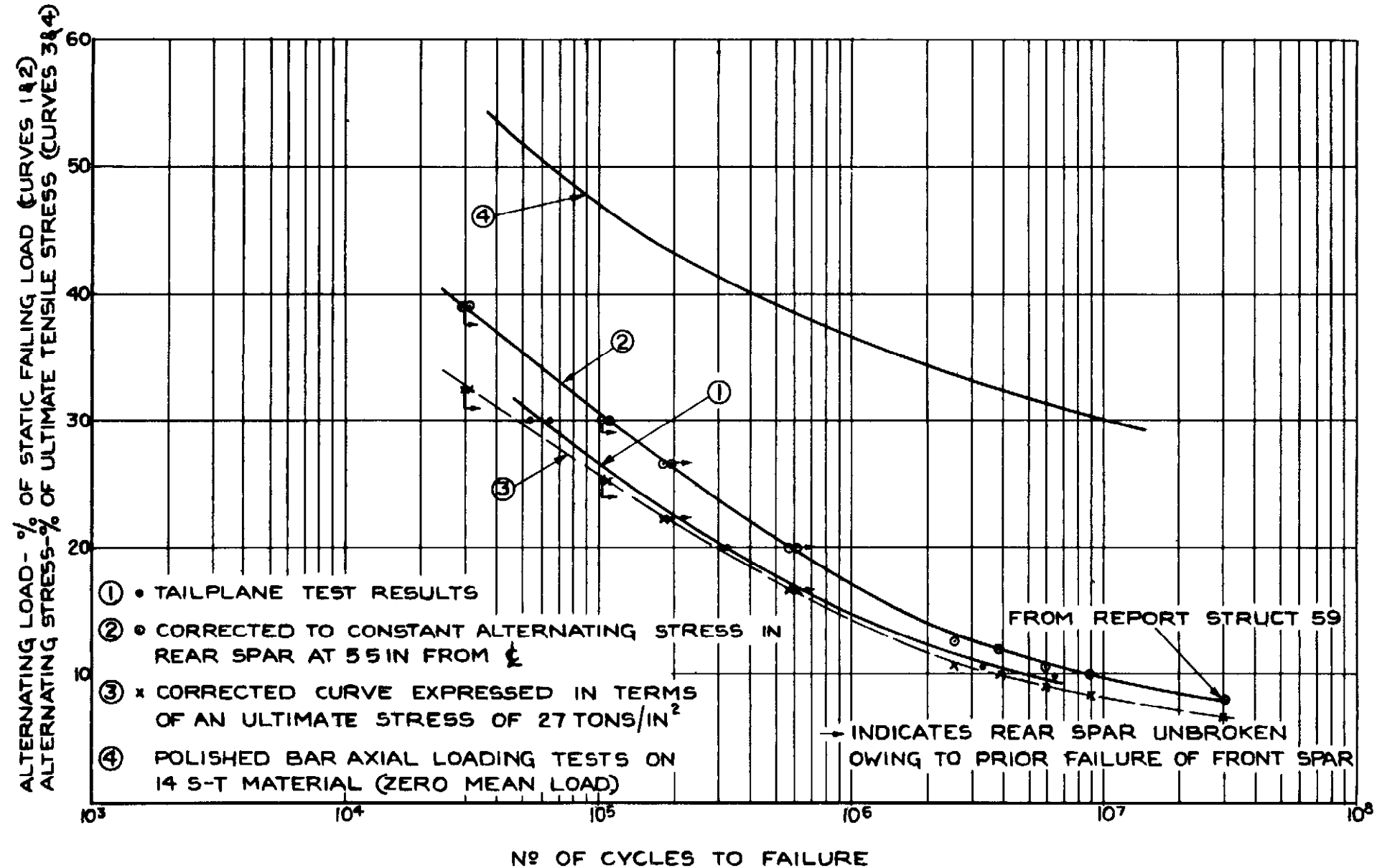

FIG.7

FIG.7. ENDURANCE CURVES FOR METEOR 4 TAILPLANE UNDER REVERSED LOADING.

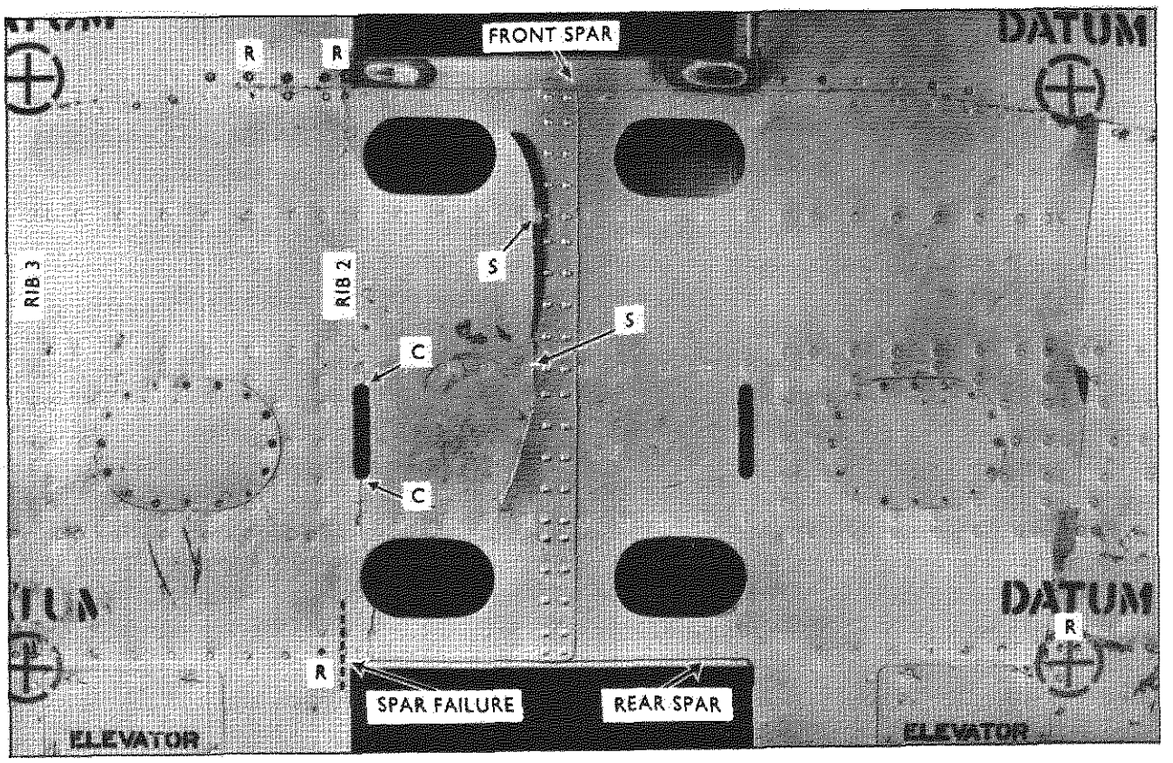

TAILPLANE No.6

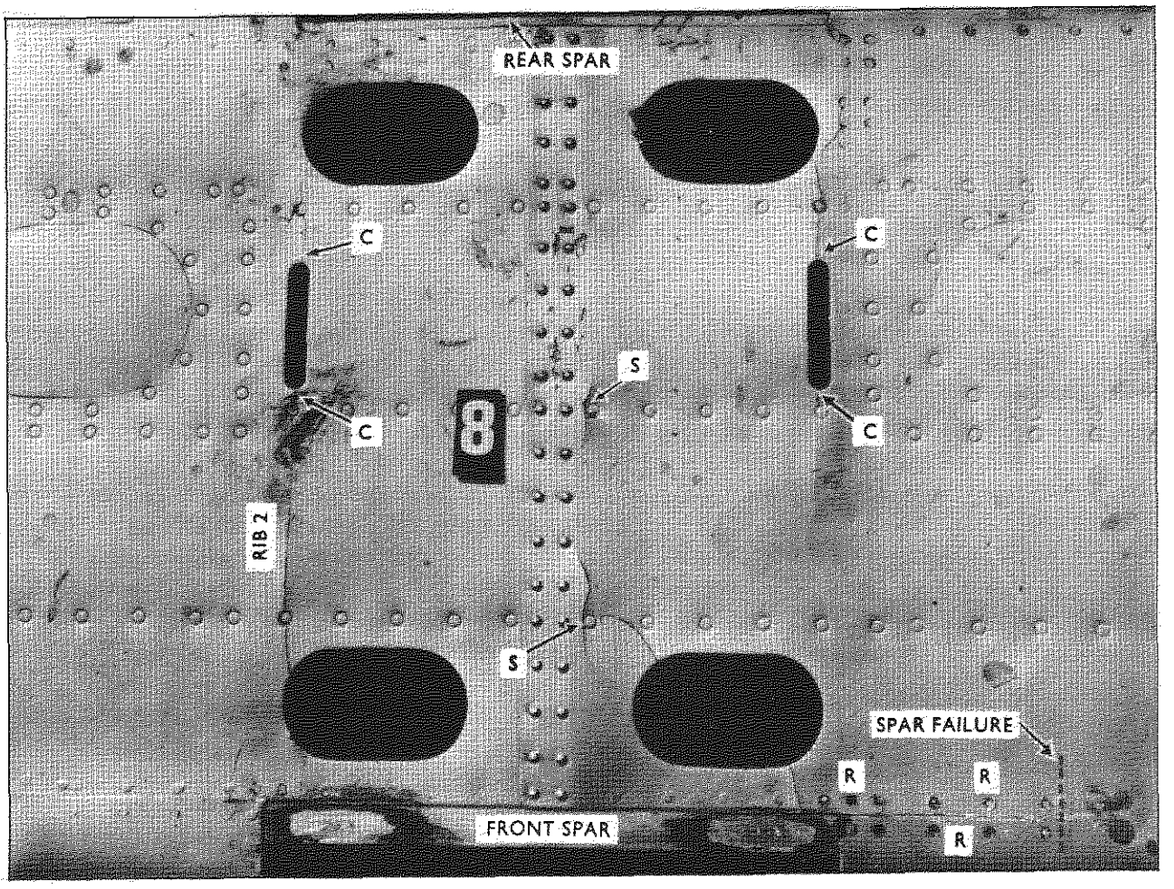

TAILPLANE No.8

C. CRACKS ORIGINATING FROM HOLES IN SKIN
S. CRACKS ORIGINATING FROM DISCONTINUOUS STRINGERS
R. RIVET FAILURES

FIG.8. TYPICAL SKIN FAILURES — UPPER SURFACE

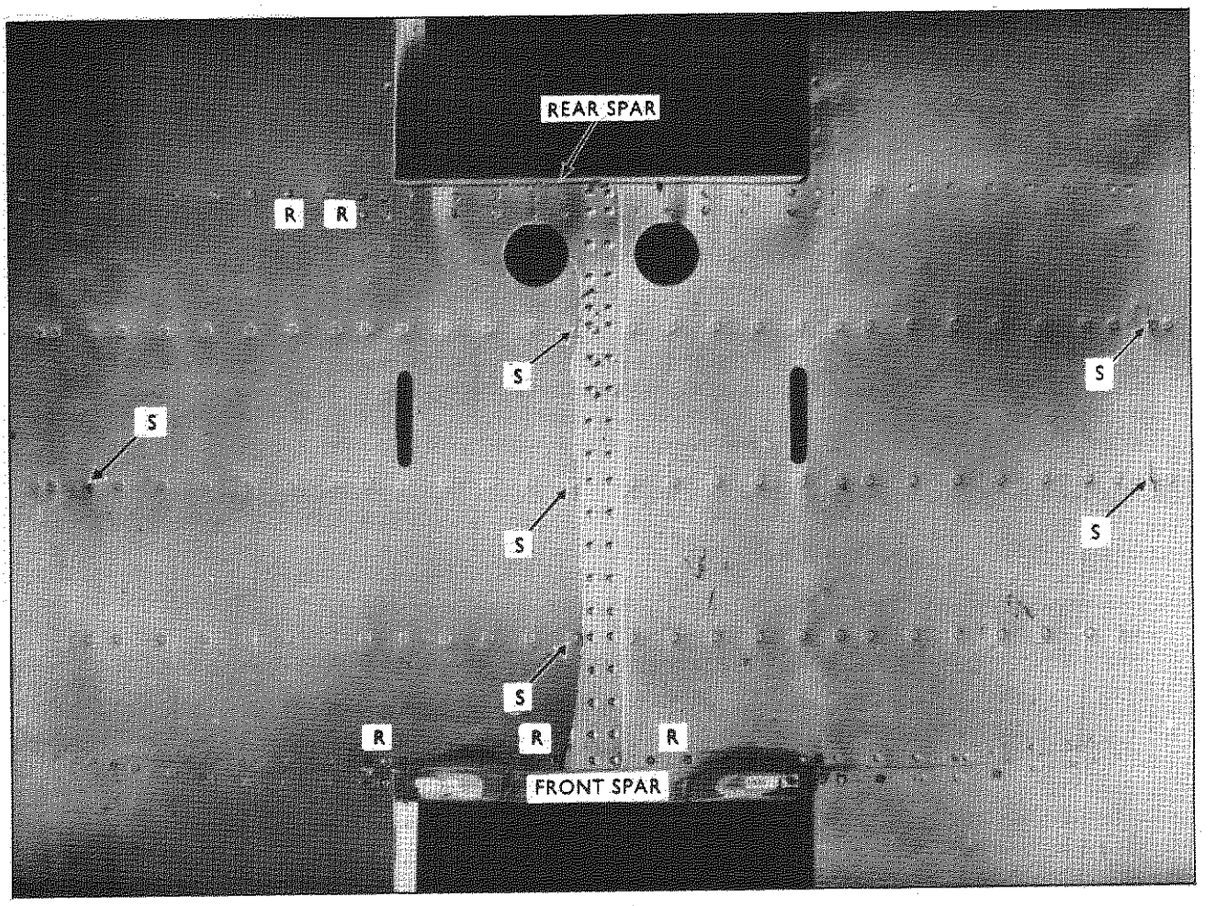

TAILPLANE No.6

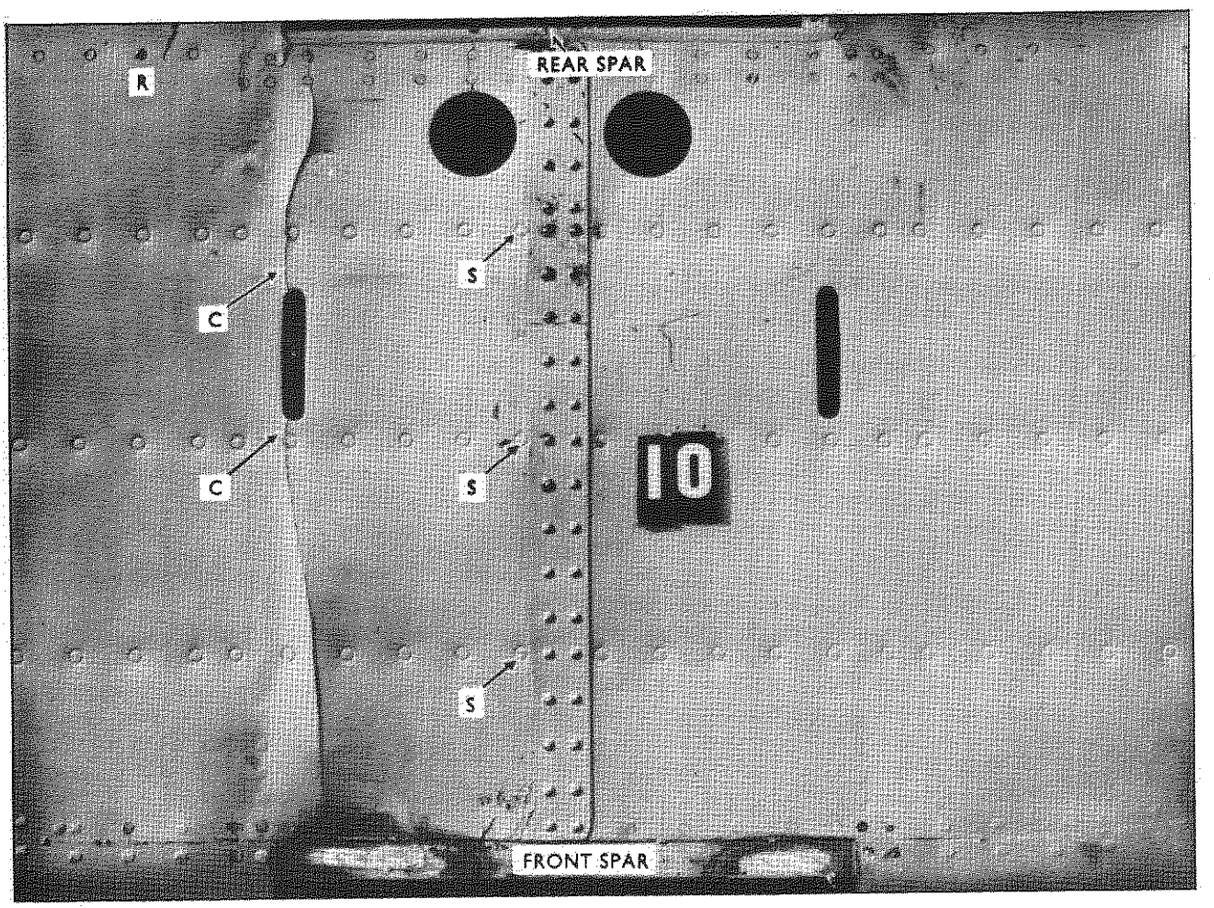

TAILPLANE No.10

C. CRACKS ORIGINATING FROM HOLES IN SKIN
S. CRACKS ORIGINATING FROM DISCONTINUOUS STRINGERS
R. RIVET FAILURES

FIG.9. TYPICAL SKIN FAILURES — LOWER SURFACE

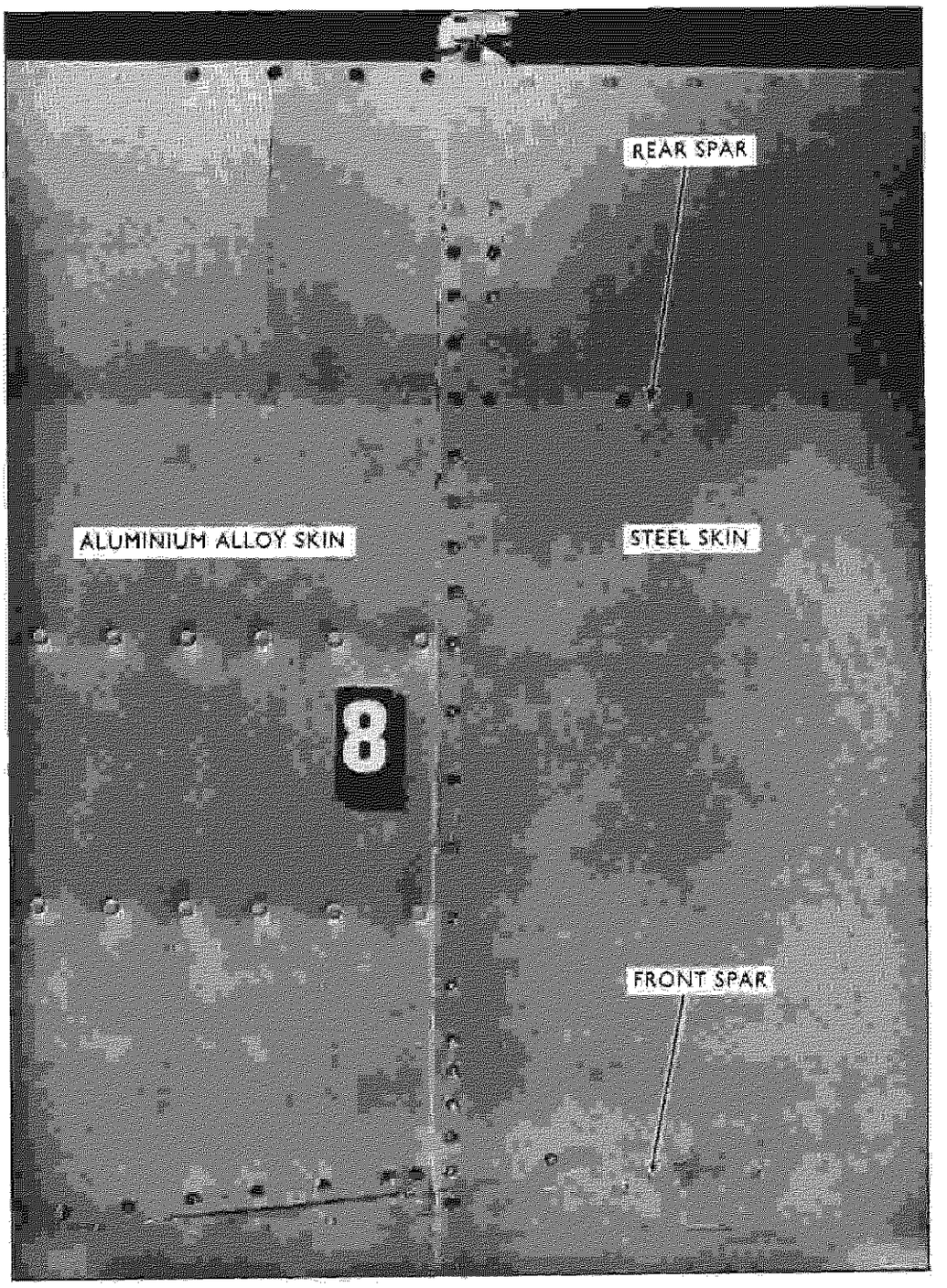

FIG.10. TYPICAL RIVET FAILURES AT RIB 5

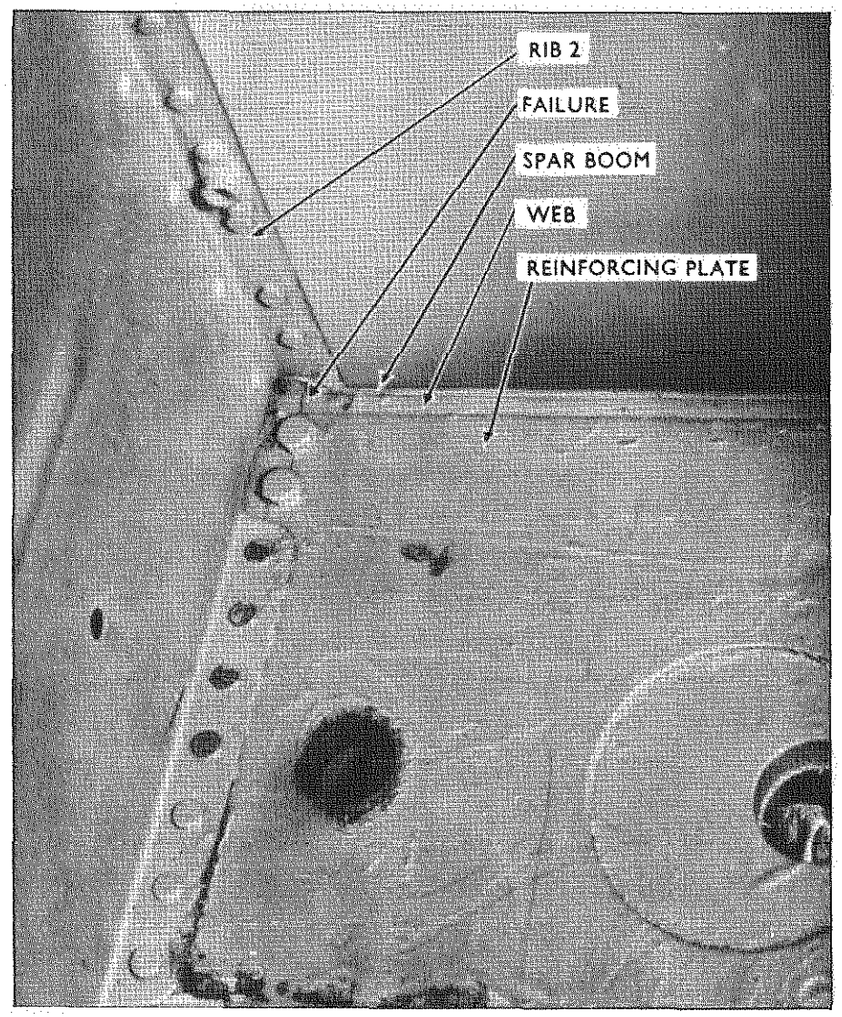

a. REAR SPAR FAILURE AT RIB 2

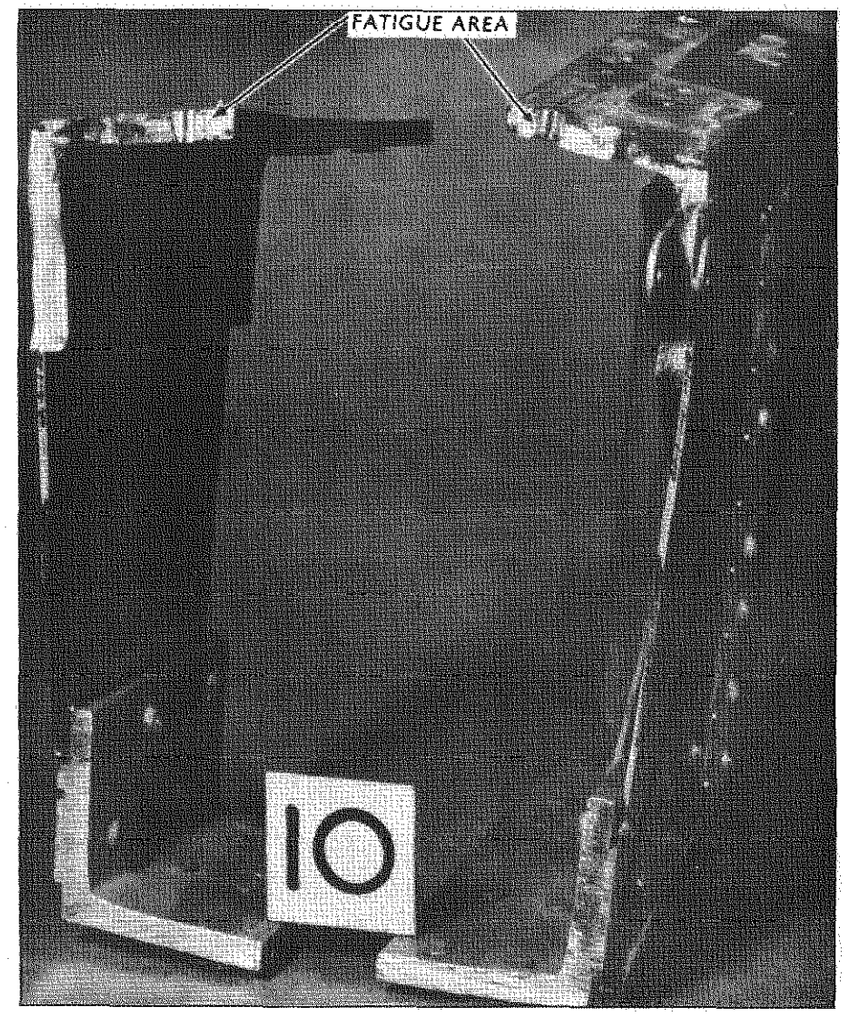

b. FRACTURED FACES OF FRONT SPAR FAILURE AT 8·5 in. FROM ℄

FIG.11. TYPICAL SPAR BOOM FAILURES

FIG. 11

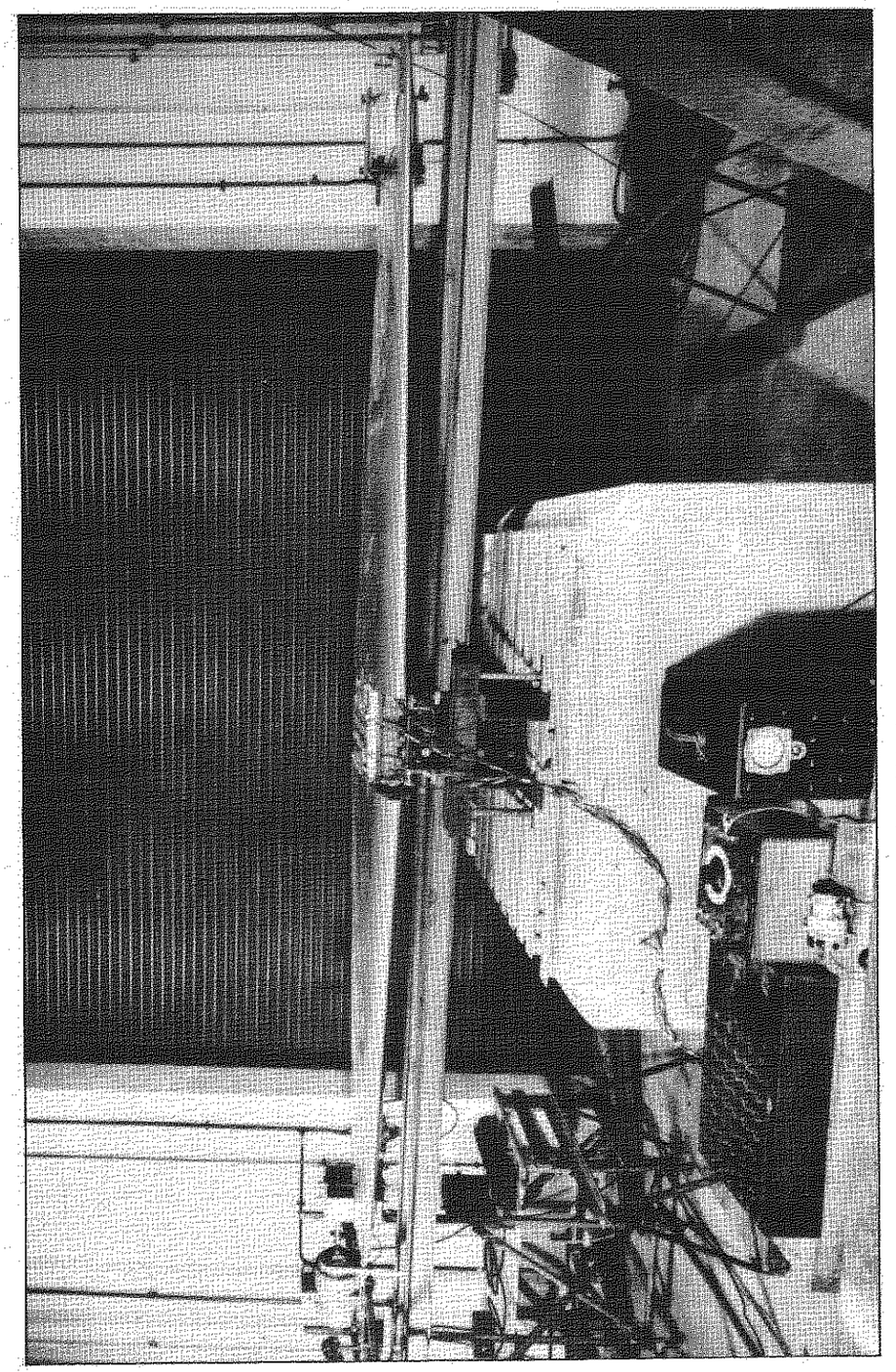

FIG.12. TAILPLANE RIGGED FOR TEST

C.P. No. 88
(14,192)
A.R.C. Technical Report

PUBLISHED BY HER MAJESTY'S STATIONERY OFFICE

To be purchased from

York House, Kingsway, LONDON, W C.2: 429 Oxford Street, LONDON, W.1
P.O Box 569, LONDON, S.E.1
13a Castle Street, EDINBURGH, 2 | 1 St. Andrew's Crescent, CARDIFF
39 King Street, MANCHESTER, 2 | Tower Lane, BRISTOL, 1
2 Edmund Street, BIRMINGHAM, 3 | 80 Chichester Street, BELFAST
or from any Bookseller

PRINTED IN GREAT BRITAIN

1952

Price 4s. 0d. net

S.O. Code No. 23-9006-88